

Decomposition of Methylbenzyl Radicals in the Pyrolysis and Oxidation of Xylenes

Gabriel da Silva*

Department of Chemical and Biomolecular Engineering, The University of Melbourne, Victoria 3010, Australia

Eric E. Moore and Joseph W. Bozzelli*

Department of Chemistry and Environmental Science, New Jersey Institute of Technology, Newark, New Jersey 07102

Received: June 18, 2009; Revised Manuscript Received: July 28, 2009

Alkyl benzyl radicals are important initial products in thermal and combustion reactions of substituted aromatic fuels. The decomposition reactions of the three isomeric methylbenzyl radicals, formed as primary products in xylene combustion, are studied theoretically and are shown to be significantly more complex than previously reported. Thermochemical properties are calculated using the G3X and G3SX model chemistries, with isodesmic and atomization work reactions. G3X atomization calculations reproduce heats of formation for the 14 reference species in the work reactions to a mean unsigned error of 0.23 kcal mol⁻¹, and maximum error of 0.70 kcal mol⁻¹, slightly outperforming the G3SX method. For the target molecules the isodesmic and atomization heats of formation agree to within 0.20 kcal mol⁻¹, on average. We posit that this study approaches the crossover point at which atomization calculations offer improved accuracy over isodesmic ones, for these closed-shell hydrocarbons. Our results suggest that *m*-xylylene is not the decomposition product of *m*-methylbenzyl, as was previously reported. Instead, the *m*-methylbenzyl radical decomposes to *p*-xylylene (and perhaps some of the less stable *o*-xylylene) via a ring-contraction/methylene-migration (RCMM) mechanism, with activation energy of around 70 kcal mol⁻¹. At higher temperatures *m*-methylbenzyl is predicted to also decompose to 2- and 3-methylfulvenallene + H, with activation energy of around 84 kcal mol⁻¹. The *o*-methylbenzyl radical is shown to primarily decompose to *o*-xylylene + H with bond dissociation energy of 67.3 kcal mol⁻¹, with fulvenallene + CH₃ proposed as a minor product set. Finally, the *p*-methylbenzyl radical decomposes solely to *p*-xylylene + H with bond dissociation energy 61.5 kcal mol⁻¹. Rate expressions are estimated for all reported reactions, based on thermochemical kinetic considerations, with further modeling along with detailed experiments needed to better refine rate constants and branching ratios for methylbenzyl radical decomposition. These calculated reaction mechanisms and rate constants for methylbenzyl radical decomposition are consistent with the experimental data. Our results help explain the ignition behavior of the xylenes, and should lead to improved kinetic models for combustion of these and other alkylated aromatic hydrocarbons.

1. Introduction

Alkylated aromatic hydrocarbons, including the xylenes, are an important component of many liquid transportation fuels. These substituted aromatics are particularly prevalent in gasoline and jet fuel formulations due to their high energy densities and resistance to autoignition (high octane ratings), and they are a promising fuel for advanced homogeneous charge compression ignition (HCCI) engines. Aromatic reactivity generally decreases with increasing ring substitution, yet the fundamental reactions governing this behavior remain unclear. The *m*-xylene research octane number (RON) of 145 is similar to that of *p*-xylene (RON = 146), and both are considerably less reactive than that of *o*-xylene (RON = 120).¹ These results are mirrored by autoignition studies,^{2,3} which show that *m*-xylene exhibits longer ignition delays than the ortho and para isomers. The large difference in reactivity between *o*-xylene and the *m*- and *p*-xylenes is commonly attributed to the presence of adjacent methyl groups, an effect observed in other alkylated aromatics.³ A smaller difference is observed between the *m*- and *p*-xylenes;

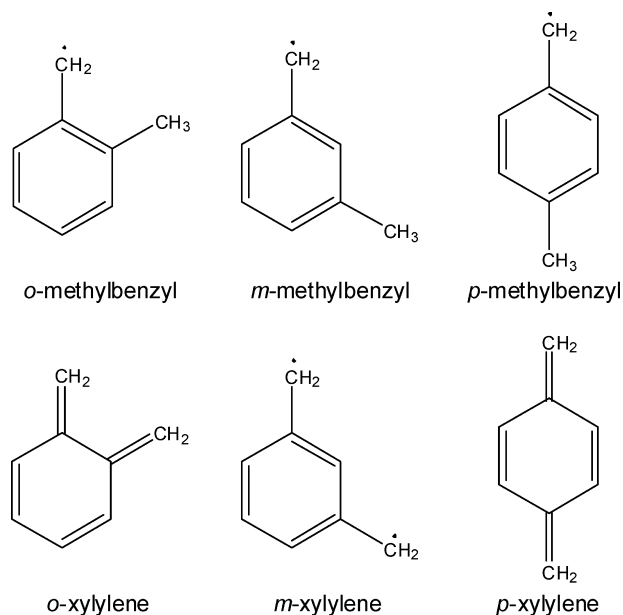
octane numbers quoted above suggest that *m*-xylene is slightly more reactive than *p*-xylene,¹ similar to the findings of Shen and Oehlschlaeger.² The autoignition study of Roubaud et al.,³ however, reports significantly increased ignition delays for *m*-xylene versus *o*-xylene at 900 K, given similar high pressures (around 20 bar). These effects remain to be explained. A thorough fundamental understanding of aromatic reactivity and oxidation chemistry is important, and this contribution continues our recent efforts in this area.^{4–10}

The initial stage of xylene decomposition primarily involves the formation of methylbenzyl radicals (Scheme 1) via unimolecular C–H fission and bimolecular H abstraction reactions. Resonantly stabilized benzyl radicals are oxidized relatively slowly in combustion systems, and unimolecular elimination reactions are therefore important, along with molecular weight growth processes including the benzyl self-reaction. Current kinetic models treat methylbenzyl radical decomposition as the loss of a second quasi-benzyl H atom, producing the bis(methylene)cyclohexadiene isomers commonly known as the xylylenes or quinodimethanes (Scheme 1).

Hippler and co-workers have studied xylene¹¹ and methylbenzyl¹² decomposition kinetics using a shock tube apparatus

* Corresponding authors. E-mail: gdasilva@unimelb.edu.au (G.S.); bozzelli@njit.edu (J.W.B.).

SCHEME 1: Methylbenzyl Radicals and Xylylenes



with atomic resonance absorption spectroscopy (ARAS) for direct H atom detection. All three xylene isomers predominantly decomposed to methylbenzyl radicals + H, with smaller amounts of C–C fission to methylphenyl radicals + CH₃. The decomposition kinetics of the methylbenzyl isomers was essentially identical, with activation energies of around 91 kcal mol⁻¹.¹¹ Further decomposition of the methylbenzyl products however, differs markedly; the activation energies were 74.1, 81.3, and 70.5 kcal mol⁻¹ for the ortho, meta, and para isomers, respectively.¹² This results in decomposition rates for the *m*-methylbenzyl radical several orders of magnitude below that for the other isomers, with a commensurate reduction in levels of free H atoms at relevant combustion temperatures. Farrell and co-workers¹³ studied laminar burning velocities for a range of fuels, and determined that these burning velocities were highly sensitive to H atom forming reactions. The peak burning velocities for *o*- and *p*-xylenes were significantly greater than that of *m*-xylene, and the increased stability of the *m*-methylbenzyl radical, versus the ortho and para isomers, was put forward as an explanation for this.^{13b}

The *m*-methylbenzyl radical is assumed to decompose to *m*-xylylene + H. *m*-Xylylene is considerably higher in energy than the ortho and para isomers, as it is unable to form a stabilizing diene ring structure (cf. Scheme 1), and instead exists as a ground state triplet diradical. The activation energy for *m*-methylbenzyl decomposition of 81.3 kcal mol⁻¹ is similar to, but still smaller than, that for decomposition of the parent benzyl radical (ca. 85 kcal mol⁻¹),^{8,14} suggesting that *m*-methylbenzyl radical decomposition in *m*-xylene combustion should play a more prominent role than benzyl decomposition in toluene combustion. The major benzyl radical decomposition products are fulvenallene + H,^{8,15} and because of the similar activation energies we hypothesize that related reactions may be taking place in *m*-methylbenzyl radical decomposition.

In this study we investigate the thermochemistry of the methylbenzyl radicals, xylylenes, and methylfulvenallenes, in order to better understand the kinetics and products of methylbenzyl radical decomposition. Our calculated thermochemistry is used to reevaluate the products and kinetics of methylbenzyl radical decomposition.

2. Computational Methods

All electronic structure calculations were performed using Gaussian 03.¹⁶ Molecules have been studied using the G3X model chemistry,¹⁷ which is based on B3LYP/6-31G(2df,p) density functional theory geometries and vibrational frequencies. The G3X energy is obtained by combining wave function theory calculations from HF through QCISD(T), using basis sets of decreasing size. Empirical corrections are added for the number of valence and unpaired electrons, and for spin-orbit coupling in the atoms. The G3X method reproduces the experimental enthalpies of formation of the G3/99 test set with a mean absolute deviation of 0.88 kcal mol⁻¹, and performs better for the hydrocarbon and radical subsets. Results are also reported here for the scaled G3X method (G3SX), which eliminates the empirical corrections for unpaired and valence electrons, but includes multiplicative scaling of the HF, second-, third-, and fourth-order MP, and QCISD(T) energy terms.¹⁷ The mean absolute deviation for the G3SX method with the G3/99 enthalpies of formation is also 0.88 kcal mol⁻¹. Optimized structures, vibrational frequencies, and energies (G3X and G3SX) for target species are provided in the Supporting Information.

Standard enthalpies of formation ($\Delta_f H^\circ_{298}$, kcal mol⁻¹), entropies (S°_{298} , cal mol⁻¹ K⁻¹), and 300–2000 K heat capacities [$C_p(T)$, cal mol⁻¹ K⁻¹] are reported for all studied species. Entropy and heat capacity calculations follow standard statistical mechanical principles, with rigid-rotor-harmonic-oscillator treatment of vibration frequencies. Internal rotational modes are treated as hindered or free rotors, based upon the results of relaxed B3LYP/6-31G(2df,p) rotor scans. Ionization energies (IEs, eV) for all ring compounds are provided in the Supporting Information, to assist with their detection in flames using tunable photoionization mass spectrometry techniques.

Enthalpies of formation are calculated using both atomization and isodesmic work reactions. In an atomization reaction the target molecule is decomposed into its constituent atoms, and the enthalpy of reaction (atomization enthalpy) is calculated using some theoretical methodology (in this case G3X or G3SX). Given experimental enthalpies of formation, we can then calculate $\Delta_f H^\circ_{298}$ of the target species. The atomization approach is beneficial for studying organic molecules in that the C and H heats of formation are relatively well-known (this study uses respective 0 K values of 169.977 and 51.634 kcal mol⁻¹),¹⁸ and that it can be readily applied to any molecule. The isodesmic approach to calculating enthalpies of formation offers potential improvements in accuracy. An isodesmic reaction is one in which the same number of each bond type appears on either side. By constructing a work reaction using reference species with accurately known heats of formation, we can obtain the target heat of formation from the calculated reaction enthalpy. Reproducing the bonding environment on either side of the reaction (through conservation of the bond types and, in practice, other interactions), systematic errors arising from the inability of the theoretical method to reproduce the true electronic structure are significantly reduced. The major proviso in the application of isodesmic work reactions is that accurate experimental heats of formation are required for all reference species, while the construction of an effective work reaction can also prove challenging. However, when useful work reactions with well-characterized reference species are used in conjunction with typical composite theoretical methods, we can calculate heats of formation that are typically twice as accurate as those from atomization reactions,¹⁹ and even greater error reduction can be achieved when using less-accurate density

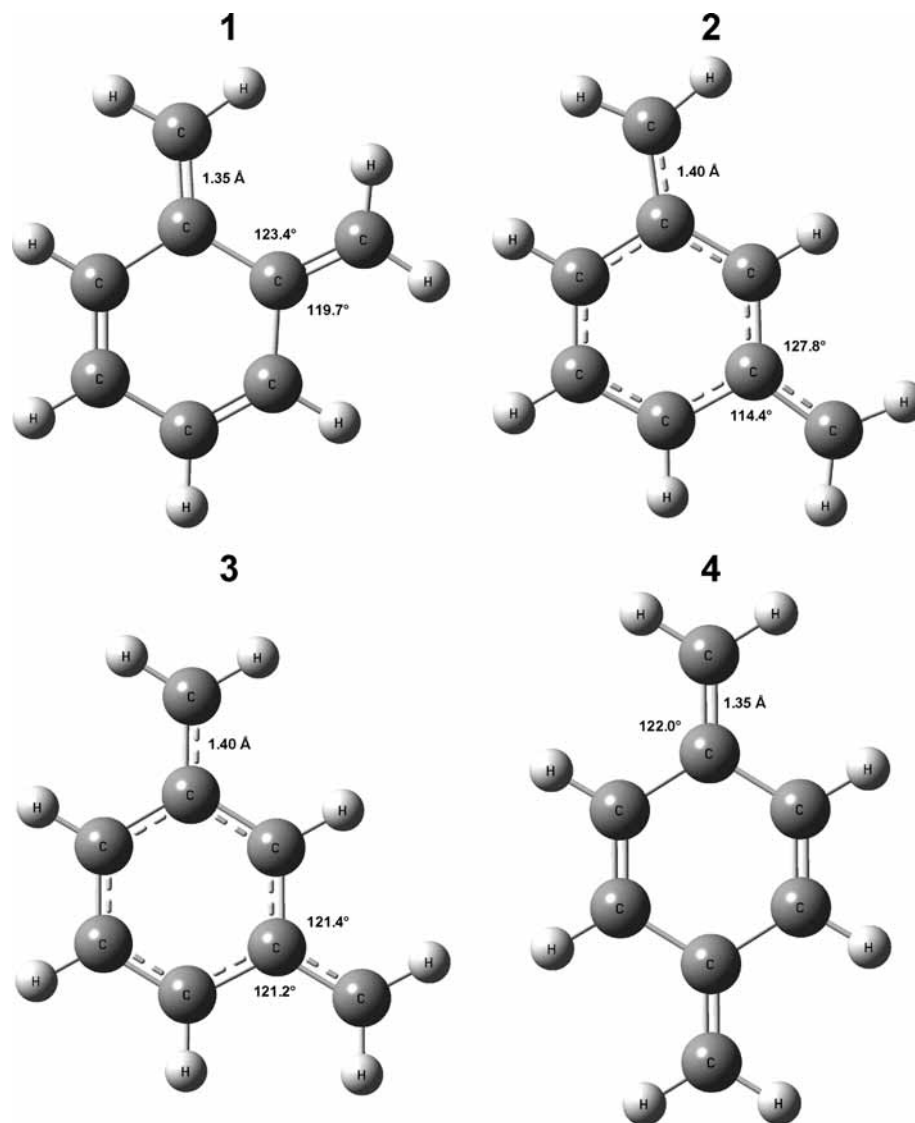


Figure 1. Optimized structures for (1) *o*-xylene, (2) singlet *m*-xylene, (3) triplet *m*-xylene, and (4) *p*-xylene, at the B3LYP/6-31G(2df,p) level.

functional theory methods. In this study we use isodesmic work reactions in calculating heats of formation for the main species of interest. Atomization heats of formation are used to check the accuracy of the isodesmic enthalpies (as large deviations between the two may indicate the use of poor reference enthalpies). Atomization enthalpies are also used to directly confirm the accuracy of reference enthalpies (at least to within the computational accuracy).

3. Results and Discussion

3.1. Optimized Structures and Internal Rotor Potentials.

In this section we consider the optimized structures for each of the target species, along with internal rotor potentials for rotation about C–CH₃ bonds. These internal rotor potentials are required to accurately determine entropy and heat capacity values, which are reported later. Optimized structures for the xylenes are depicted in Figure 1, with the methylbenzyl radicals in Figure 2 and the fulvenallenes in Figure 3. Important bond lengths and angles have been included in the figures; full structures are available in the Supporting Information.

The xylenes all have 2-fold symmetry (symmetry point groups are C_2 for *o*-xylene, C_{2v} for singlet and triplet *m*-xylene, and D_{2h} for *p*-xylene), and bond lengths and angles

for each methylene group in these molecules are therefore the same. With *o*-xylene there is a significant steric effect caused by the adjacent methylene groups, which are distorted to be above and below the plane of the ring (see side-on depiction in the Supporting Information). This result is expected to explain the difference in kinetics for *o*-methylbenzyl versus *p*-methylbenzyl decomposition, and should be reflected in the xylene thermochemistry. The C=CH₂ distances in *o*-xylene are essentially the same as those in *p*-xylene (all 1.35 Å). In the *m*-xylenes the C–CH₂ distances are significantly increased over the ortho and meta isomers, reflecting the lone pair/unpaired electron sites. In triplet *m*-xylene the CH₂ groups are essentially perpendicular to the C₆ ring, while in the singlet configuration they are significantly distorted (although still planar, given the C_{2v} symmetry).

The methylbenzyl radical structures are depicted in Figure 2, and changes between the three isomers are relatively minor. In *o*-methylbenzyl the adjacent methyl group does interact with the benzyl radical site to some extent, but this has little effect on the energy (vide infra). All structures obey the C_s symmetry point group, with C atoms lying in a plane. In the *o*- and *m*-methylbenzyl radicals a H atom in the methyl group eclipses the benzene ring, while in *p*-methylbenzyl it is staggered. This

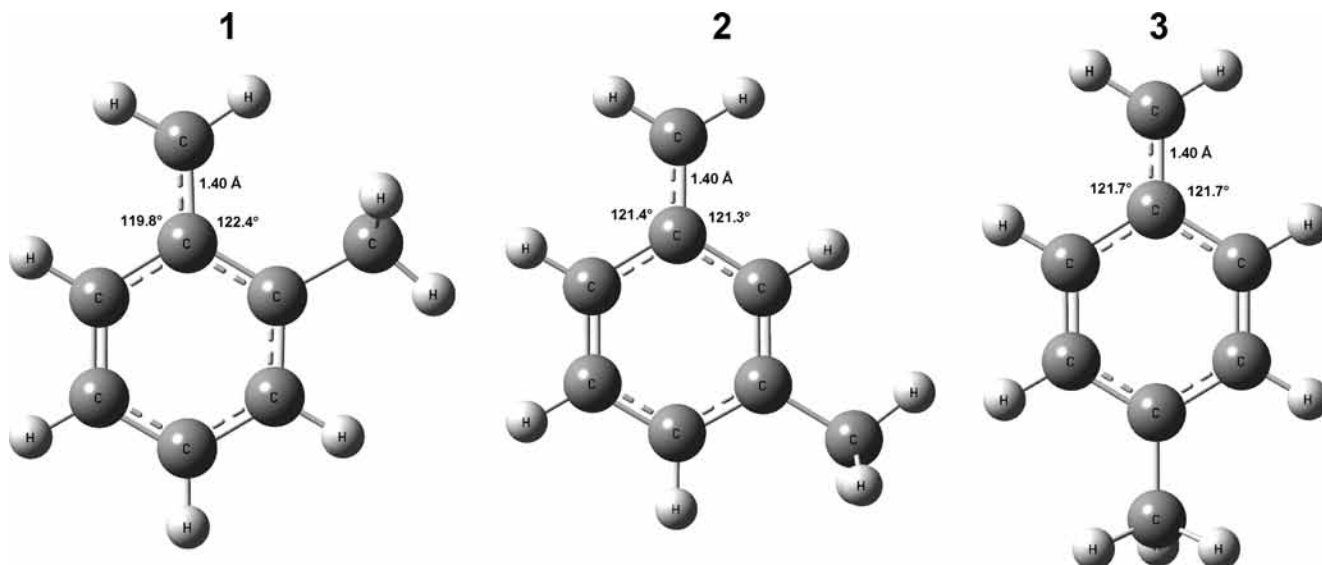


Figure 2. Optimized structures for (1) *o*-methylbenzyl, (2) *m*-methylbenzyl, and (3) *p*-methylbenzyl, at the B3LYP/6-31G(2df,p) level.

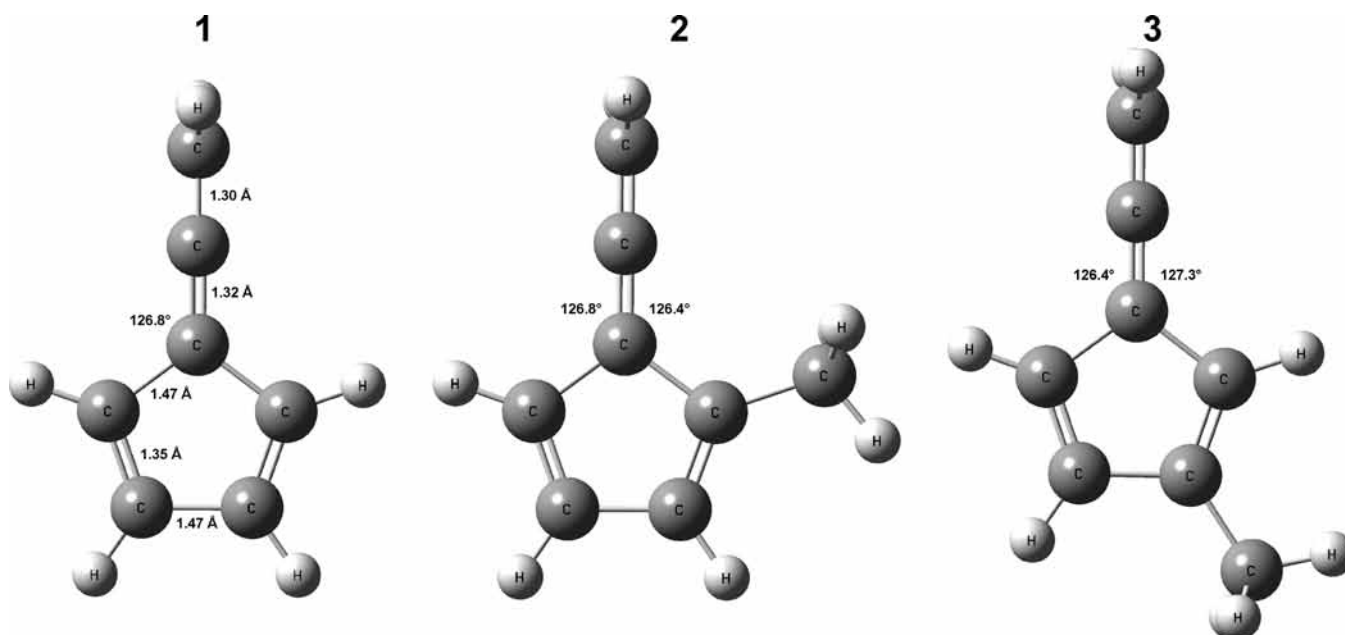


Figure 3. Optimized structures for (1) fulvenallene, (2) 2-methylfulvenallene, and (3) 3-methylfulvenallene, at the B3LYP/6-31G(2df,p) level.

results in a 6-fold rotor for the *p*-methylbenzyl radical (with minima occurring when each H atom is either above or below the ring), with 3-fold rotors for the other isomers (Figure 4). Additionally, the rotational barrier in the para isomer ($0.01 \text{ kcal mol}^{-1}$) is much lower than in the ortho and meta isomers (1.9 and $0.2 \text{ kcal mol}^{-1}$, respectively); this appears to be one of the lowest barriers ever reported for internal rotation about a carbon–carbon bond. The increase in barrier for methyl rotation in *o*-methylbenzyl is a result of the $\text{CH}_3\cdots\text{C}\cdot\text{H}_2$ interaction. The C–C rotor in the *p*-methylbenzyl radical corresponds to a 27 cm^{-1} vibration, and this mode is treated as a free rotor. The *o*- and *m*-methylbenzyl radical internal rotors correspond to 155 and 58 cm^{-1} vibrations, respectively, and are treated using a hindered rotor model.

The methylfulvenallenes are similar in structure to fulvenallene (Figure 3), with all carbon–carbon bonds being approximately equal in length (and therefore not included in the structure diagrams for 2- and 3-methylfulvenallenes). Hyperconjugation arising from introduction of the methyl group does

distort the C_5 ring to some extent, but the molecules retain C_s symmetry (introduction of the methyl group clearly breaks the C_{2v} symmetry point group of fulvenallene). Internal rotor potentials for the methylfulvenallenes are depicted in Figure 5. The methyl groups generate 3-fold rotor potentials with minima corresponding to eclipsed configurations. Internal rotation in 3-methylfulvenallene requires around $1.3 \text{ kcal mol}^{-1}$, while 2-methylfulvenallene needs only $0.8 \text{ kcal mol}^{-1}$. This effect is the result of the 2-methylfulvenallene minima being slightly destabilized relative to 3-methylfulvenallene (higher-level calculations later reveal this energy difference to be around $0.2 \text{ kcal mol}^{-1}$), whereas the rotational maxima have essentially the same electronic energy.

3.2. Work Reactions. Standard enthalpies of formation for the xylylenes are determined using isodesmic work reactions, along with calculated G3X reaction enthalpies and literature reference heats of formation. In total, four work reactions are used for each *o*-xylylene and *p*-xylylene, where two feature cyclohexadiene ring structures and two feature benzene ring

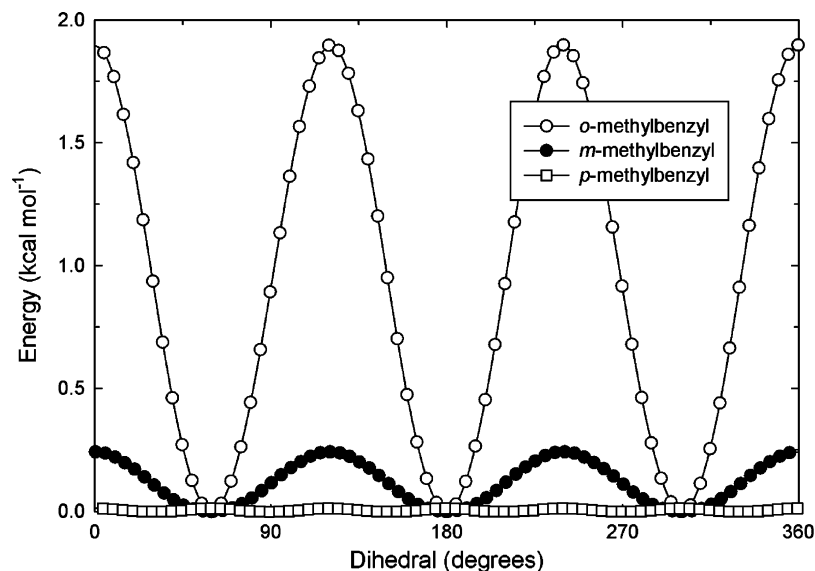


Figure 4. Internal C–CH₃ rotor potentials in the methylbenzyl radicals. Calculated at the B3LYP/6-31G(2df,p) level of theory. Detail of the low-energy *p*-methylbenzyl internal rotor (barrier = 0.013 kcal mol⁻¹) is provided in the Supporting Information.

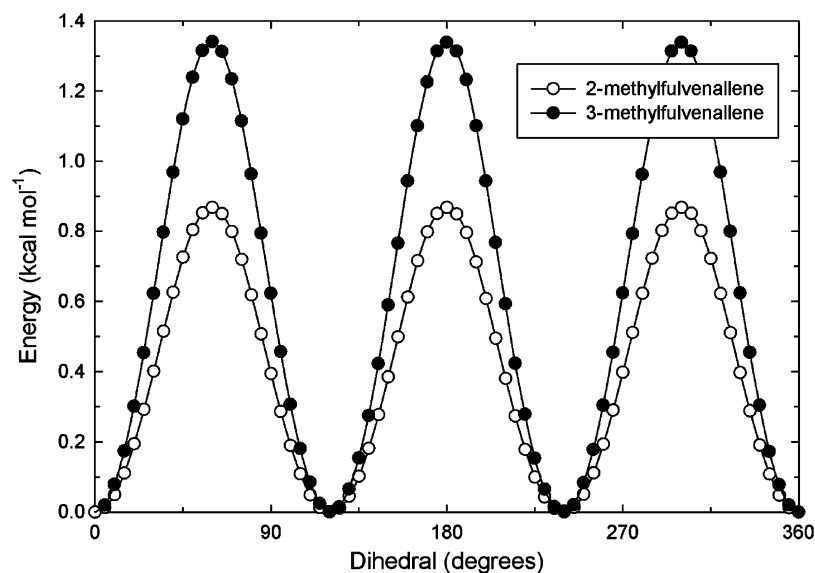
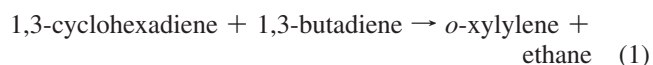


Figure 5. Internal C–CH₃ rotor potentials in 2- and 3-methylfulvenallenes. Calculated at the B3LYP/6-31G(2df,p) level of theory.

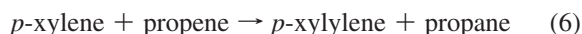
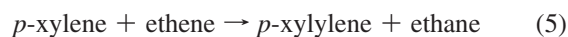
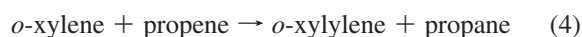
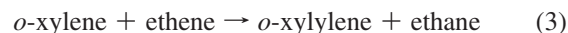
structures. The true xylylene structure is expected to lie somewhere between the two.

The first set of work reactions (eqs 1 and 2) use 1,3-cyclohexadiene and 1,4-cyclohexadiene to model the diene ring structures in *o*-xylylene and *p*-xylylene, respectively. The double bonds to the methylene groups are described using 1,3-butadiene. The cyclohexadienes should be good models for the xylylene ring structures, although additional stabilization is expected in the xylylenes, as all carbon–carbon double bonds are conjugated.

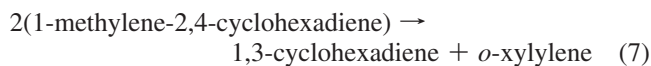


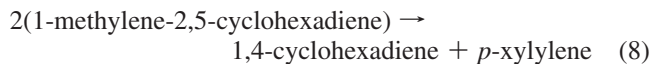
The second set of work reactions (eqs 3–6) utilize *o*- and *p*-xylenes to model the xylylene ring structures, with ethene or propene included to describe the additional carbon–carbon

double bond. These work reactions are expected to be endothermic, due to the loss of resonance in the xylenes, but should provide a better representation of the fully conjugated xylylene ring structures.

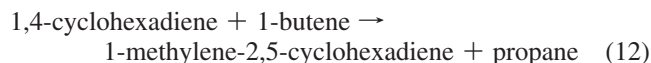
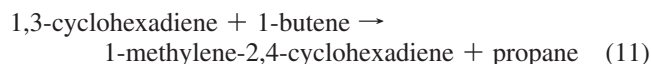
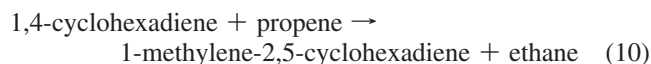
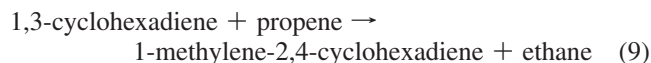


The final set of work reactions for *o*- and *p*-xylylene (eqs 7 and 8) make use of the methylenecyclohexadienes, along with the cyclohexadienes used in reactions 1 and 2:

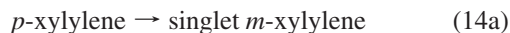
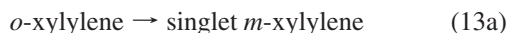




Reactions 7 and 8 are expected to provide improved error cancellation over reactions 1 and 2, due to inclusion of one conjugated methylene group in the methylenecyclohexadienes. However, in the course of this study we identify that the methylenecyclohexadiene heats of formation are not well-known (vide infra). As such, these enthalpies are also determined here, using the following isodesmic work reactions:



Because *m*-xylylene does not possess a conjugated diene ring structure, it is difficult to describe using the above work reaction approach. Instead, for *m*-xylylene we calculate the heat of formation using reactions 13a/13b and 14a/14b, along with the *o*- and *p*-xylylene heats of formation arrived at using the above work reaction schemes. This approach is applied to both singlet (eqs 13a and 14a) and triplet (eqs 13b and 14b) *m*-xylylene.



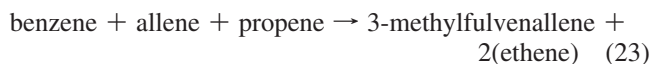
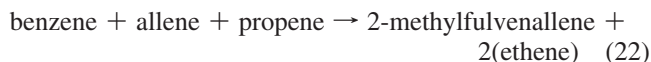
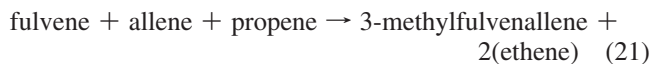
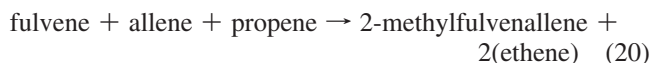
Similarly, nonisodesmic work reactions are applied to calculate the methylbenzyl radical heats of formation. Application of an isodesmic approach to calculating a radical heat of formation requires an accurately known bond dissociation energy for formation of a similar radical. The best models for loss of a benzyl H atom in the xylylenes are C₆H₅CH₂-H dissociation in toluene and CH₂CHCH₂-H dissociation in propene, but there remain significant uncertainties in these bond dissociation energies, and we elect not to use them here. Instead, methylbenzyl radical heats of formation are calculated using bond dissociation work reactions, which should still provide considerable error cancellation over the atomization reactions. The bond dissociation work reactions are given below (eqs 15–17), and we see that the radical heats of formation can be precisely calculated given accurate values for the xylene heats of formation.



In this study we propose that fulvenallenes can be important products in the decomposition of substituted benzyl radicals. The importance of fulvenallene as a combustion intermediate has only recently been realized, and in the absence of experimental thermochemistry, accurate computational values are of value. Here, we determine the fulvenallene heat of formation using the following isodesmic work reactions:



The benzene aromaticity is lost in reaction 19, as with reactions 3–6, leading to less error cancellation than in reaction 18. However, the benzene heat of formation is known to much greater precision than that of fulvene, and the use of benzene provides an internal check on the fulvene reference heat of formation. The 2- and 3-methylfulvenallenes are studied using the following related work reactions:



3.3. Literature and Atomization Enthalpies. Literature heats of formation have been compiled for each of the reference species in the above work reactions, along with values for the target species. Literature values are generally taken from the Active Thermochemical Tables,²⁰ where available. In addition to the literature values, we have calculated heats of formation for each species using an atomization methodology, at the G3X level. Atomization calculations generally do not attain the accuracy of isodesmic calculations, due to the lack of error cancellation across the atomization work reaction. However, because atomization calculations use only accurate experimental heats of formation, they are not susceptible to the large errors that can be introduced by using poorly known reference heats of formation. In this way the atomization calculations provide a sanity check on the heats of formation used for the reference species, and on those obtained from the isodesmic calculations.

Table 1 compares the atomization (G3X and G3SX) and literature heats of formation for all species invoked in this study. For the 14 reference species (excluding the methylenecyclohexadienes) agreement between the literature and atomization enthalpies is exceptional for the G3X method, with a mean unsigned error of only 0.23 kcal mol⁻¹ and a maximum error of 0.70 kcal mol⁻¹. The mean signed error is close to zero (+0.03 kcal mol⁻¹), indicating little systematic bias in the G3X atomization calculations. The G3SX calculations provide similar

TABLE 1: Standard Enthalpies of Formation ($\Delta_f H^\circ_{298}$) for Target and Reference Species in the Present Study

	$\Delta_f H^\circ_{298}$ (kcal mol ⁻¹)		
	G3X	G3SX	literature
ethane	-20.08	-20.22	-20.03 ²⁰
propane	-24.97	-25.19	-25.02 ²⁰
ethene	12.40	12.18	12.57 ²⁰
propene	4.81	4.58	4.84 ²⁰
1-butene	0.15	-0.15	-0.01 ²⁰
1,3-butadiene	26.61	26.27	26.49 ²⁰
1,3-cyclohexadiene	26.11	26.11	25.41 ²⁰
1,4-cyclohexadiene	26.17	26.27	26.05 ²⁰
<i>o</i> -xylene	3.96	4.05	4.54 ²¹
<i>m</i> -xylene	4.12	4.38	4.12 ²¹
<i>p</i> -xylene	4.46	4.65	4.29 ²¹
1-methylene-2,4-cyclohexadiene	43.99	43.84	35 ²²
1-methylene-2,5-cyclohexadiene	40.04	39.90	35, ²² 46.99 ²³
allene	45.00	44.71	45.48 ²⁰
fulvene	51.68	51.79	51.17 ²⁴
benzene	20.27	20.47	20.34 ²⁰
fulvenallene	84.19	84.32	–
2-methylfulvenallene	75.28	75.40	–
3-methylfulvenallene	75.06	75.20	–
<i>o</i> -xylylene	59.07	58.71	53, ²⁵ 60.8 ²⁶
<i>m</i> -xylylene (singlet)	96.01	93.40	–
<i>m</i> -xylylene (triplet)	79.33	79.66	>76, ²⁵ 80.8 ²⁷
<i>p</i> -xylylene	52.78	52.49	50 ²⁵
<i>o</i> -methylbenzyl	43.25	42.75	40.01 ²⁸
<i>m</i> -methylbenzyl	43.23	42.80	40.01 ²⁸
<i>p</i> -methylbenzyl	43.34	42.92	40.01 ²⁸

results to G3X, where the mean unsigned error is now 0.33 kcal mol⁻¹, with a maximum deviation of 0.77 kcal mol⁻¹ and a mean unsigned error of -0.04 kcal mol⁻¹. All further calculations reported here refer only to the G3X method, as it provides the superior results in these atomization calculations.

Agreement of the atomization enthalpies with the literature values confirms the high accuracy of the G3X model chemistry, and also suggests that experimental heats of formation for all reference species are accurately known. When a C atom 0 K heat of formation of 170.122 kcal mol⁻¹²⁹ is used in the atomization calculations (from the Active Thermochemical Tables), instead of 169.977 kcal mol⁻¹, the mean unsigned error for the G3X heats of formation slips to 0.75 kcal mol⁻¹, with a maximum error of 1.57 kcal mol⁻¹. Interestingly, the mean signed error is also 0.75 kcal mol⁻¹, with the calculated heats of formation all larger than or equal to the experimental values, a clear systematic deviation. Our results make no comment on the correct, fundamental heat of formation of the carbon atom (or $H_{298} - H_0$), but do strongly suggest that a value of 169.977 kcal mol⁻¹ (with $H_{298} - H_0 = 0.251$ kcal mol⁻¹) should be used in G3X atomization calculations.

For fulvene we have adopted a reference heat of formation of 51.17 kcal mol⁻¹ (taken from a recent critical evaluation/computational study),²⁴ which is considerably lower than the commonly used experimental value of 53.6 kcal mol⁻¹. Our G3X atomization calculations return a fulvene heat of formation of 51.68 kcal mol⁻¹, in excellent agreement with the more recent value. Further support for this lower fulvene heat of formation comes from high-level ab initio calculations by Karton et al.,³⁰ using the post-CCSD(T) W3.2lite method. Here, the 0 K fulvene heat of formation was evaluated as 55.12 ± 0.5 kcal mol⁻¹, while our G3X 0 K value is 55.55 kcal mol⁻¹. The W3.2lite calculations also provide a benzene heat of formation of 23.96 ± 0.4 kcal mol⁻¹ at 0 K, whereas G3X theory yields a value of 24.48 kcal mol⁻¹. The agreement between the G3X and W3.2lite calculations is encouraging, although larger discrepancies may

arise for radicals. Recently we applied G3X theory in evaluating the phenyl radical 0 K heat of formation as 85.60 kcal mol⁻¹,⁹ whereas the W3.2lite calculations result in a value of 83.35 ± 0.5 kcal mol⁻¹.³⁰ Modern experimental measurements of this value are typically larger than, but within combined experimental and theoretical uncertainty of, the W3.2lite value.³¹

For the methylenecyclohexadienes our calculated heats of formation are in considerable disagreement with the available literature values. The 1-methylene-2,5-cyclohexadiene heat of formation is calculated to be 40.04 kcal mol⁻¹, intermediate to the literature values which range from 46.99 to 35 kcal mol⁻¹. This 35 kcal mol⁻¹ value was also proposed for 1-methylene-2,4-cyclohexadiene, which we find to be somewhat less stable than 1-methylene-2,5-cyclohexadiene ($\Delta_f H^\circ_{298} = 43.99$ kcal mol⁻¹). For the methylbenzyl radicals and the xylylenes, the main targets of this study, we find significant differences between our calculated enthalpies of formation and some of the quoted literature values. The discrepancies in the literature justify our theoretical reevaluation of these thermochemical properties. To our knowledge no experimental values are available for singlet *m*-xylylene, fulvenallene, or the methylfulvenallenes.

3.4. Isodesmic Enthalpies of Formation. Enthalpies of formation have been evaluated for the target species using the work reactions described in section 3.1, at the G3X level. Calculated reaction enthalpies for each of the work reactions are listed in Table 2, along with the evaluated heat of formation for the target species. Recommended heats of formation from work reactions are listed in Table 3, where they are the average across all reactions. Atomization heats of formation are included for comparison. In Table 2 we see that the enthalpy change across the isodesmic work reactions is generally small (excluding the bond dissociation reactions 15–17), indicative of good bond energy and error cancellation.

With *o*- and *p*-xylylene we find that the reaction enthalpies are positive for those work reactions involving the xylenes as reference species (3–6), and negative for those involving cyclohexadiene reference species (1, 2, 7, 8), signifying respective over- and underprediction of the total xylylene bond energy. The best reference species for the xylylenes appear to be the methylenecyclohexadienes, as we achieve very small reaction enthalpies for reactions 7 and 8. If we use 1,3-cyclohexadiene in place of 1,4-cyclohexadiene in eq 1, and vice versa for eq 2, then the *o*- and *p*-xylylene heats of formation are calculated to be 58.78 and 51.92 kcal mol⁻¹, respectively. These values are consistent with those obtained from the other work reactions, and the choice of cyclohexadiene isomer used to model the different xylylenes is probably insignificant.

For fulvenallene and the methylfulvenallenes the work reactions using fulvene achieve near-complete bond energy cancellation. In this context the relative success of group additivity at reproducing the fulvenallene heat of formation is not surprising (82 kcal mol⁻¹).³² Good agreement for the fulvenallene enthalpies with the work reactions using fulvene and with those using benzene provide further support for a fulvene heat of formation in the range of about 51–52 kcal mol⁻¹.

The isodesmic and atomization heats of formation from this study agree to within a mean unsigned error of 0.20 kcal mol⁻¹ and maximum error of 0.76 kcal mol⁻¹ (this excludes the methylbenzyl and *m*-xylylene heats of formation, which are not technically obtained using isodesmic work reactions). The mean signed error between the isodesmic and atomization enthalpies is -0.17 kcal mol⁻¹, versus a mean unsigned error of 0.20 kcal

TABLE 2: Reaction Enthalpies ($\Delta_r H^\circ_{298}$) and Target Species Heats of Formation ($\Delta_f H^\circ_{298}$) for Thermodynamic Work Reactions^a

no.	reaction	$\Delta_r H^\circ_{298}$	$\Delta_f H^\circ_{298}$
1	1,3-cyclohexadiene + 1,3-butadiene \rightarrow <i>o</i>-xylylene + ethane	-13.73	58.20
2	1,4-cyclohexadiene + 1,3-butadiene \rightarrow <i>p</i>-xylylene + ethane	-20.07	52.50
3	<i>o</i> -xylene + ethene \rightarrow <i>o</i>-xylylene + ethane	22.62	59.76
4	<i>o</i> -xylene + propene \rightarrow <i>o</i>-xylylene + propane	25.32	59.72
5	<i>p</i> -xylene + ethene \rightarrow <i>p</i>-xylylene + ethane	15.84	52.73
6	<i>p</i> -xylene + propene \rightarrow <i>p</i>-xylylene + propane	18.54	52.69
7	2(1-methylene-2,4-cyclohexadiene) \rightarrow 1,3-cyclohexadiene + <i>o</i>-xylylene	-2.81	58.24
8	2(1-methylene-2,5-cyclohexadiene) \rightarrow 1,4-cyclohexadiene + <i>p</i>-xylylene	-1.13	52.54
9	1,3-cyclohexadiene + propene \rightarrow 1-methylene-2,4-cyclohexadiene + ethane	-7.01	43.27
10	1,4-cyclohexadiene + propene \rightarrow 1-methylene-2,5-cyclohexadiene + ethane	-11.02	39.90
11	1,3-cyclohexadiene + 1-butene \rightarrow 1-methylene-2,4-cyclohexadiene + propane	-7.23	43.19
12	1,4-cyclohexadiene + 1-butene \rightarrow 1-methylene-2,5-cyclohexadiene + propane	-11.24	39.82
13a	<i>o</i> -xylene \rightarrow singlet <i>m</i>-xylylene	36.95	95.93
13b	<i>o</i> -xylene \rightarrow triplet <i>m</i>-xylylene	20.26	79.24
14a	<i>p</i> -xylene \rightarrow singlet <i>m</i>-xylylene	43.23	95.84
14b	<i>p</i> -xylene \rightarrow triplet <i>m</i>-xylylene	26.55	79.16
15	<i>o</i> -xylene \rightarrow <i>o</i>-methylbenzyl + H	91.40	43.83
16	<i>m</i> -xylene \rightarrow <i>m</i>-methylbenzyl + H	91.22	43.23
17	<i>p</i> -xylene \rightarrow <i>p</i>-methylbenzyl + H	90.98	43.17
18	fulvene + allene \rightarrow fulvenallene + ethene	-0.08	84.00
19	benzene + allene \rightarrow fulvenallene + ethene	31.32	84.57
20	fulvene + allene + propene \rightarrow 2-methylfulvenallene + 2(ethene)	-1.41	74.94
21	fulvene + allene + propene \rightarrow 3-methylfulvenallene + 2(ethene)	-1.62	74.73
22	benzene + allene + propene \rightarrow 2-methylfulvenallene + 2(ethene)	30.00	75.52
23	benzene + allene + propene \rightarrow 3-methylfulvenallene + 2(ethene)	29.79	75.31

^a In kcal mol⁻¹. Target species in bold.

TABLE 3: Isodesmic and Atomization Enthalpies of Formation

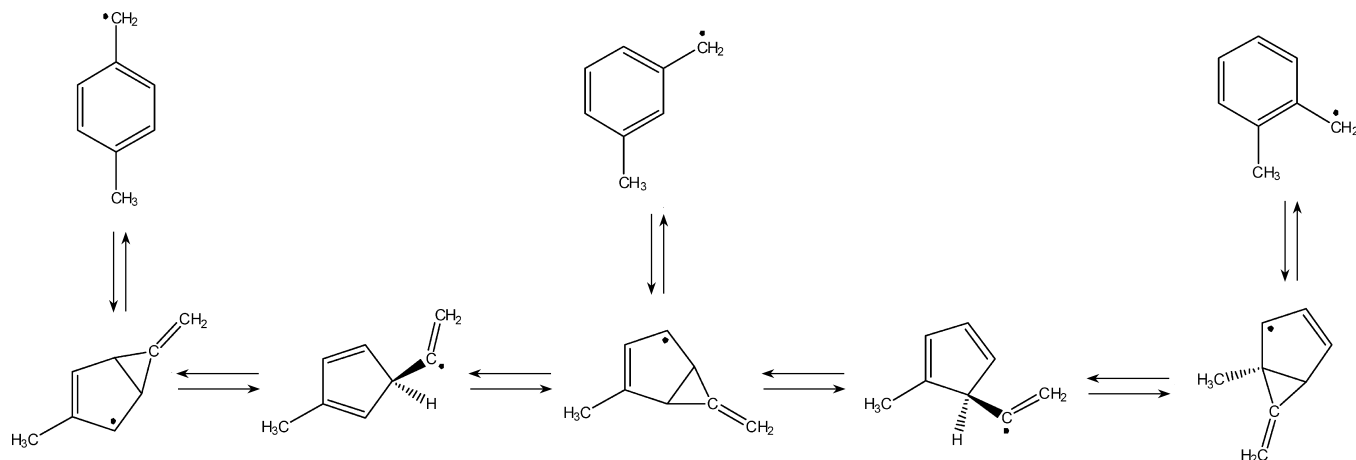
	$\Delta_f H^\circ_{298}$ (kcal mol ⁻¹)	
	isodesmic	atomization
<i>o</i> -xylylene	58.98	59.07
singlet <i>m</i> -xylylene	95.89	96.01
triplet <i>m</i> -xylylene	79.20	79.33
<i>p</i> -xylylene	52.61	52.78
1-methylene-2,4-cyclohexadiene	43.23	43.99
1-methylene-2,5-cyclohexadiene	39.86	40.04
<i>o</i> -methylbenzyl	43.83	43.25
<i>m</i> -methylbenzyl	43.23	43.23
<i>p</i> -methylbenzyl	43.17	43.34
fulvenallene	84.29	84.19
2-methylfulvenallene	75.23	75.28
3-methylfulvenallene	75.02	75.06

mol⁻¹, as the atomization enthalpies are generally larger than the isodesmic ones. While it is possible to trace this back to the C atom reference enthalpy, this small discrepancy for these molecules with seven to eight carbon atoms corresponds to a per-carbon difference of only 0.02 kcal mol⁻¹. Agreement between the atomization and isodesmic target heats of formation is similar to that between the atomization and literature reference heats of formation (mean unsigned error of 0.23 kcal mol⁻¹). It is therefore difficult for us to conclude that in this instance the painstaking application of isodesmic work reactions has offered any increase in accuracy over the atomization ones, given their already excellent performance.

As we have discussed before,^{19c} as the level of theory is increased there is expected to come a point at which atomization heats of formation actually offer improved accuracy over

isodesmic ones, and we may be approaching that point in this study. In both isodesmic and atomization heats of formation the uncertainty consists of two components: experimental (due to the reference heats of formation) and computational (due to the theoretical method, error cancellation across the work reaction, etc). The advantage to atomization calculations is that the experimental component of the uncertainty is almost always small (and smaller than for similar isodesmic calculations), and the total uncertainty largely reflects the accuracy of the theoretical method. With the atomization approach the computational error will almost always be larger than when using isodesmic work reactions; however, as the accuracy of the theoretical method is increased the computational uncertainties will become similar, in relative terms, while the experimental uncertainties remain unchanged. Accordingly, a crossover point should exist where the combined computational and experimental error for isodesmic calculations becomes larger than that for atomization calculations. It appears to us that, at least for the relatively simple hydrocarbons investigated here, this crossover point occurs for methodologies of accuracy similar to that of G3X. We should state however that the usefulness of isodesmic work reactions in calculating thermochemical properties of larger molecules that are not so amenable to high-level theoretical methods remains unquestioned.

Our best calculated heat of formation for *o*-xylylene is 58.98 kcal mol⁻¹, in close agreement with the experimental value from ref 26. The value of 53 kcal mol⁻¹ reported by Pollack et al.²⁵ appears to be in error. The calculated *p*-xylylene enthalpy is 52.61 kcal mol⁻¹, which is considerably higher than the available experimental measurement (50 kcal mol⁻¹).²⁵ For ground state *m*-xylylene we obtain a heat of formation of 79.20 kcal mol⁻¹,

SCHEME 2: Interconversion of the Methylbenzyl Radicals via the Ring-Contraction/Methylene-Migration (RCMM) Mechanism


which is close to the experimental number of $80.8 \text{ kcal mol}^{-1}$ reported by Hammad and Wenthold,²⁷ and conforms to the assignment of Pollack et al. ($>76 \text{ kcal mol}^{-1}$). For singlet *m*-xylylene we calculate the heat of formation to be $95.89 \text{ kcal mol}^{-1}$, providing a singlet–triplet gap of $16.69 \text{ kcal mol}^{-1}$; to our knowledge neither of these values has been reported previously.

For the methylenecyclohexadienes, which were used in our work reactions, we calculate isodesmic heats of formation that differ significantly from the available experimental values. The 1-methylene-2,4-cyclohexadiene enthalpy is $43.23 \text{ kcal mol}^{-1}$, while for 1-methylene-2,5-cyclohexadiene it is $39.86 \text{ kcal mol}^{-1}$. Bartmess assigned heats of formation of 35 kcal mol^{-1} to both methylenecyclohexadienes,²² while Bally et al.²³ determined a value of $46.99 \text{ kcal mol}^{-1}$ for 1-methylene-2,5-cyclohexadiene.

The methylbenzyl radical heats of formation determined using the bond dissociation and the atomization work reactions are all around $43\text{--}44 \text{ kcal mol}^{-1}$, $3\text{--}4 \text{ kcal mol}^{-1}$ higher than the experimental values of Hayashibara et al.²⁸ For the *o*-methylbenzyl radicals the bond dissociation and atomization values are in disagreement, and this can be attributed to the experimental *o*-xylene heat of formation,²¹ which is considerably higher than that of the other xylenes. The atomization calculations also support an *o*-xylene heat of formation that is somewhat lower than the experimental value. This enthalpy may need to be reevaluated in the future, although the computational accuracy of our calculations is not sufficient to state definitively that the *o*-xylene heat of formation is in error.

The final target molecules in our thermochemical evaluations are the fulvenallenes, for which experimental heats of formation are unavailable. As mentioned above, the fulvenallene heat of formation has been calculated as 82 kcal mol^{-1} from group additivity,³² compared to our isodesmic value of $84.29 \text{ kcal mol}^{-1}$. Previously, we obtained a G3X atomization heat of formation of $85.20 \text{ kcal mol}^{-1}$ for fulvenallene, using an alternate value for the C atom heat of formation.²⁹ Using our new fulvenallene enthalpy, with an experimental benzyl heat of formation of $51.5 \pm 1.0 \text{ kcal mol}^{-1}$,³³ the reaction enthalpy for decomposition of benzyl to fulvenallene + H is calculated as $84.9 \text{ kcal mol}^{-1}$. This is the same as the G3X reaction enthalpy reported previously.⁸

Using an average methylbenzyl radical heat of formation of $43.2 \text{ kcal mol}^{-1}$, and a value of $35.05 \text{ kcal mol}^{-1}$ for the methyl radical,³⁴ we calculate an enthalpy change of $76.1 \text{ kcal mol}^{-1}$ for the methylbenzyl \rightarrow fulvenallene + CH_3 reaction. The

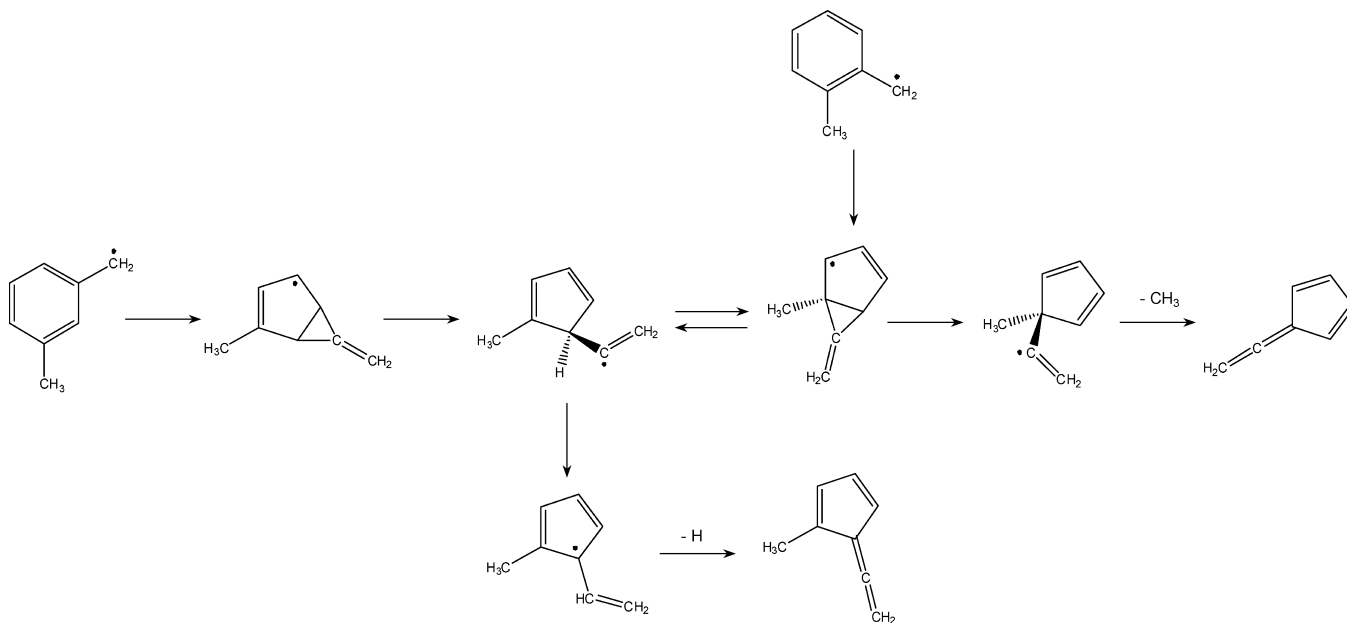
methylfulvenallene isomers are similar in energy, with 3-methylfulvenallene the more stable of the two. Decomposition of the methylbenzyl radicals to 3-methylfulvenallene + H requires around $83.9 \text{ kcal mol}^{-1}$, similar to the analogous reaction in benzyl, but significantly greater than the required reaction enthalpy for the formation of fulvenallene + CH_3 .

In the following sections the accurate thermochemical properties reported above are used to further investigate the products and kinetics of methylbenzyl radical decomposition.

3.5. Methylbenzyl Pyrolysis. Currently, the methylbenzyl radicals are considered to decompose only to their respective xylenes (+ H), via C–H β -scission reactions. Here, we propose several alternate mechanisms that seem to be of some significance. Kinetic expressions are estimated for these processes, and comparisons made to experiment, in the following sections.

The first mechanism involves interconversion of the three methylbenzyl isomers, as illustrated in Scheme 2. This is termed the ring-contraction/methylene-migration (RCMM) mechanism, and follows the initial stages of benzyl radical decomposition.^{8,15} In the first step the aromatic ring contracts to a fused $\text{C}_5\text{--C}_3$ bicyclic compound, where the barrier is expected to be around 61 kcal mol^{-1} . Following this, the methylene group can move around the molecule by opening the three-membered ring and then reforming it at another C site on the five-membered ring. The barrier for this second step should be around 70 kcal mol^{-1} above the methylbenzyl radical,⁸ and will be the rate-determining step in the RCMM isomerization process. While the overall RCMM barrier is large relative to the activation energy for *p*-methylbenzyl decomposition to *p*-xylylene, it appears to be competitive with decomposition of the other isomers.

A second alternate mechanism is decomposition of the methylbenzyl radicals to fulvenallene + CH_3 and to 2- and 3-methylfulvenallenes + H. Scheme 3 depicts pathways to these product sets from the *o*- and *m*-methylbenzyl radicals. The *p*-methylbenzyl radical can similarly decompose to 3-methylfulvenallene, or can access the reactions of Scheme 3 via the RCMM mechanism. The cyclopentadiene-type intermediate formed from *o*-methylbenzyl isomerization can undergo C– CH_3 homolysis to produce fulvenallene; if the C–C dissociation reaction proceeds without any intrinsic barrier, then the total barrier to form fulvenallene + CH_3 will be around 75 kcal mol^{-1} . Scheme 3 also shows how intermediates formed from *m*-methylbenzyl can produce 2-methylfulvenallene + H. By analogy to benzyl radical decomposition, this reaction has a

SCHEME 3: Pathways to Fulvenallene and 2-Methylfulvenallene in the Pyrolysis of the *o*- and *m*-Methylbenzyl Radicals^a


^a The *p*-methylbenzyl radical can similarly decompose to 3-methylfulvenallene + H, or access the above reactions via RCMM isomerization to *m*-methylbenzyl.

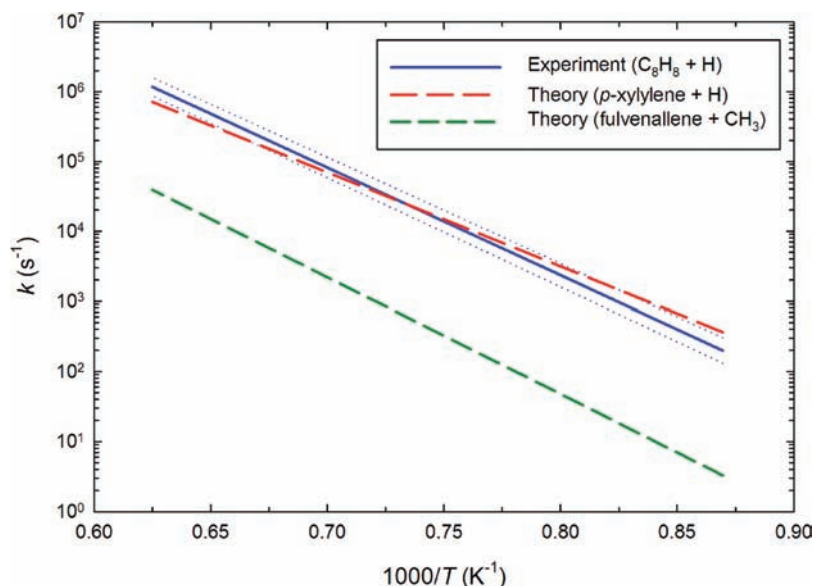


Figure 6. Experimental and estimated rate constants for thermal decomposition of the *p*-methylbenzyl radical. Dotted lines represent experimental uncertainties.

thermodynamic barrier of 83.9 kcal mol⁻¹.⁸ The *p*-methylbenzyl isomers will decompose similarly to 3-methylfulvenallene ($\Delta_r H^\circ_{298} = 84.0$ kcal mol⁻¹), and all of the methylbenzyl radicals can isomerize with each other according to Scheme 2.

The importance of the above mechanisms, as well as traditional decomposition to the xylylenes, is considered for methylbenzyl radical decomposition in the following sections.

3.5.1. *p*-Methylbenzyl Radical Decomposition. Now we consider the kinetics of *p*-methylbenzyl decomposition, which should follow the simplest mechanism of the three isomers. The *p*-methylbenzyl decomposition rate expression of Fernandez et al.¹² is plotted in Figure 6 (dotted lines indicate their assigned uncertainty in E_a). From our suggested thermochemistry we find that the enthalpy change for the reaction *p*-methylbenzyl \rightarrow *p*-xylylene + H is 61.5 kcal mol⁻¹, significantly smaller than

the Fernandez et al.¹² activation energy of 70.5 kcal mol⁻¹. If we approximate the decomposition rate constant as $k [s^{-1}] = A \exp[(-\Delta_r H^\circ_{298} - RT)/(RT)]$, and fit this expression to the experimental data in ref 12, we obtain an activation energy of 61.5 kcal mol⁻¹ and a pre-exponential factor of $1.8 \times 10^{14} s^{-1}$. The experimental and fitted rate constants then agree to within the experimental uncertainty (see Figure 6). A pre-exponential factor of around $10^{14} s^{-1}$ is entirely reasonable for a C–H β -scission reaction, although considerably smaller than the value of $5 \times 10^{15} s^{-1}$ expected by Fernandez et al.¹² The higher pre-exponential factors assigned to methylbenzyl radical decomposition in ref 12 may be the result of using too-large activation energies, while the fitted value reported here may be low due to falloff effects. Fernandez et al.¹² estimated falloff as reducing the observed methylbenzyl decomposition rate constants by

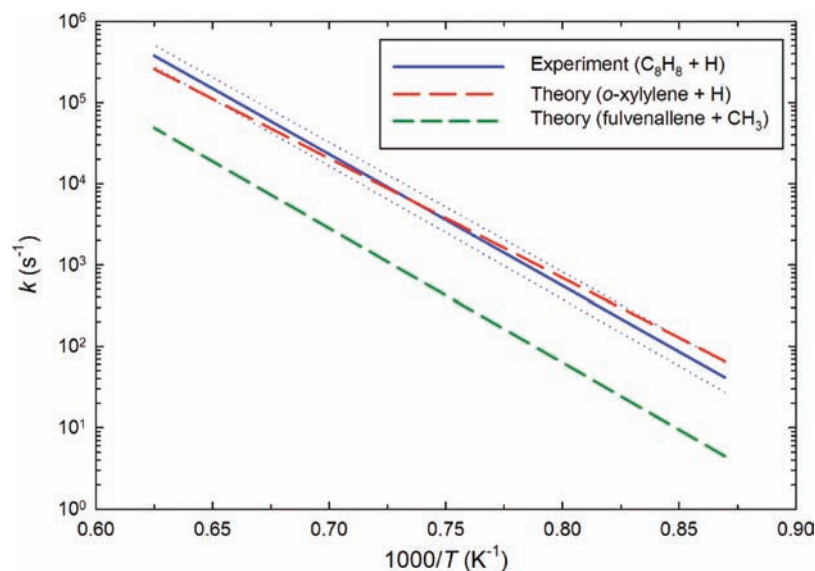


Figure 7. Experimental and estimated rate constants for thermal decomposition of the *o*-methylbenzyl radical. Dotted lines represent experimental uncertainties.

about a factor of 4, and this would result in an extrapolated high-pressure-limit pre-exponential factor of $7.2 \times 10^{14} \text{ s}^{-1}$ for *p*-methylbenzyl decomposition, based upon our work.

An alternate product set in *p*-methylbenzyl radical decomposition is fulvenallene + CH_3 , where the reaction enthalpy is $76.2 \text{ kcal mol}^{-1}$ (when using a CH_3 heat of formation of $34.821 \text{ kcal mol}^{-1}$). We use an activation energy of $76.2 \text{ kcal mol}^{-1}$ for this reaction, while the pre-exponential factor is conservatively estimated as $1 \times 10^{15} \text{ s}^{-1}$ (ca. $4 \times 10^{15} \text{ s}^{-1}$ in the high-pressure limit). Dissociation of a C–C bond is entropically favored over C–H bond dissociation, with pre-exponential factors that are typically around an order of magnitude larger (cf. toluene decomposition),³⁵ and it is likely that the fulvenallene + CH_3 product set increases in importance with increasing temperature. It may, however, be the case that this dissociation reaction proceeds via an adiabatic transition state, with a small barrier above the reaction enthalpy. In this case the activation energy will increase somewhat, and the tighter transition state structure would be expected to decrease the pre-exponential factor. Estimated rate constants for the fulvenallene + CH_3 channel are included in Figure 6, and we expect these products to only account for around 2–5% of total *p*-methylbenzyl decomposition at relevant combustion temperatures. We should note that the fulvenallene + CH_3 decomposition products could not have been detected by Fernandez et al., as they followed reaction progress by studying H atom evolution.

3.5.2. *o*-Methylbenzyl Radical Decomposition. Our calculations indicate that the thermodynamic barrier for *o*-methylbenzyl decomposition to *o*-xyllylene + H is considerably greater than that for the similar reaction in *p*-methylbenzyl. This finding is reflected in the experimental results of Fernandez et al.,¹² where the activation energy for *o*-methylbenzyl decomposition was $74.1 \text{ kcal mol}^{-1}$, around 4 kcal mol^{-1} greater than that for *p*-methylbenzyl decomposition. Our calculations suggest that the barrier for *o*-methylbenzyl radical decomposition is $67.3 \text{ kcal mol}^{-1}$, nearly 6 kcal mol^{-1} higher than the corresponding reaction in *p*-methylbenzyl. Using our calculated reaction enthalpy, and following the same procedure as above, we obtain the rate expression $k [\text{s}^{-1}] = 4.0 \times 10^{14} \exp(-33900/T)$. This estimated rate expression is plotted in Figure 7, along with the experimental data, and again we find that the two expressions approximately agree to within the experimental uncertainty. The

pre-exponential factor of $4.0 \times 10^{14} \text{ s}^{-1}$ is also closer to the empirical value of $5 \times 10^{15} \text{ s}^{-1}$ used by Fernandez et al.¹² Extrapolating our results to the high-pressure limit, we obtain an approximate pre-exponential factor of $1.6 \times 10^{15} \text{ s}^{-1}$, a value typical for C–H bond dissociation.

For *o*-methylbenzyl decomposition we again consider fulvenallene + CH_3 as potential reaction products. The *o*-methylbenzyl barrier to *o*-xyllylene is considerably larger than with the para isomer, and these products are now expected to play a greater role. The activation enthalpy for *o*-methylbenzyl decomposition to fulvenallene + CH_3 is estimated as $75.5 \text{ kcal mol}^{-1}$, and a pre-exponential factor of $1 \times 10^{15} \text{ s}^{-1}$ is again used. The approximated rate expression is plotted in Figure 7; we now see that rate constants for formation of this product set are only around an order of magnitude below those for *o*-xyllylene at these relatively moderate temperatures. We predict that fulvenallene + CH_3 constitute around 10–15% of the *o*-methylbenzyl decomposition products, comprising a relatively important product set. Detailed kinetic calculations are required to better refine the rate expression for formation of fulvenallene + CH_3 . Additionally, the proposed mechanism would also be supported by the detection of elevated levels of fulvenallene in *o*-xyllylene flames (versus *p*-xyllylene).

3.5.3. *m*-Methylbenzyl Radical Decomposition. Experimentally, the *m*-methylbenzyl radical decomposes to a C_8H_8 species + H with activation energy of $81.3 \text{ kcal mol}^{-1}$. The barrier for *m*-methylbenzyl radical decomposition is considerably greater than that for the ortho and para isomers, and this has historically been attributed to the formation of triplet *m*-xyllylene. However, our results suggest that the activation enthalpy for formation of triplet *m*-xyllylene + H from *m*-methylbenzyl is $88.1 \text{ kcal mol}^{-1}$. This is considerably larger than the experimental activation energy, especially when one considers that the calculated reaction enthalpies for decomposition of the ortho and para isomers were all much smaller than the corresponding experimental activation energies. The experimental rate constant expression for *m*-methylbenzyl radical decomposition to a C_8H_8 species + H is plotted in Figure 8, along with an estimated expression from our work. Here, the activation energy has been set to $88.1 \text{ kcal mol}^{-1}$, and an average pre-exponential factor of $2.8 \times 10^{14} \text{ s}^{-1}$ is used, based upon our above results. We find that the estimated rate constants for *m*-methylbenzyl

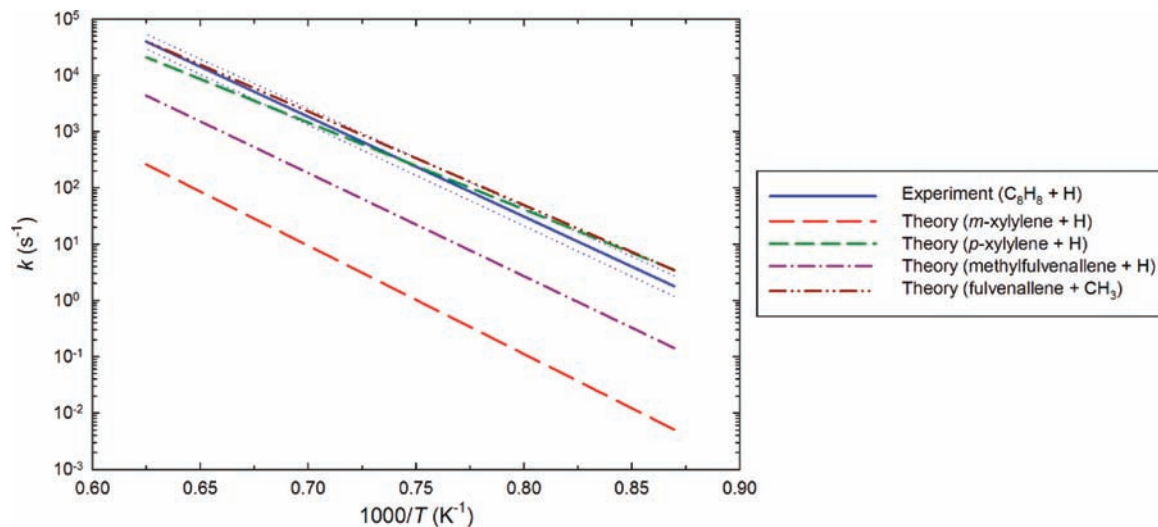
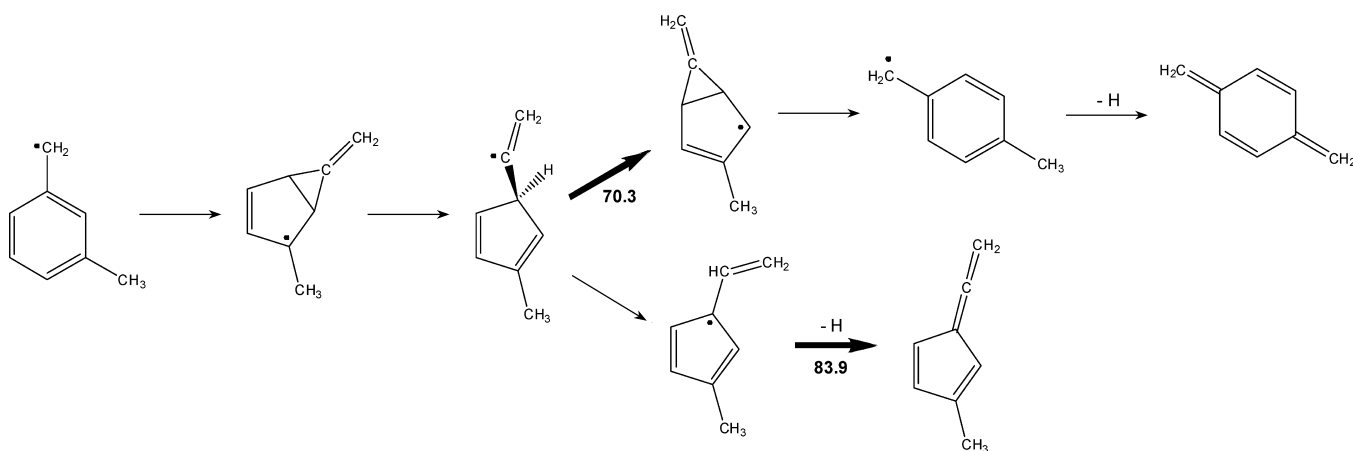


Figure 8. Experimental and estimated rate constants for thermal decomposition of the *m*-methylbenzyl radical. Dotted lines represent experimental uncertainties.

SCHEME 4: Proposed Decomposition Mechanism for the *m*-Methylbenzyl Radical to C₈H₈ + H^a



^a The rate-determining step in each reaction channel is in bold, along with the estimated enthalpy of activation (in kcal mol⁻¹). Similar pathways to the higher energy isomers *o*-xylylene and 2-methylfulvenallene also exist.

decomposition to *m*-xylylene are far below the measured values (almost 3 orders of magnitude), and we therefore suggest that triplet *m*-xylylene is not the observed C₈H₈ decomposition product of the *m*-methylbenzyl radical. It is possible that the pre-exponential factor for *m*-methylbenzyl decomposition to *m*-xylylene is considerably larger than that for the ortho and para isomers, but it would have to be a physically unrealistic value of around 10¹⁷–10¹⁸ s⁻¹ for these products to dominate. As with the ortho and para isomers, we consider the importance of fulvenallene + CH₃ as decomposition products of *m*-methylbenzyl, but this reaction produces the methyl radical, and is therefore unable to explain the formation of C₈H₈ + H.

We propose that the C₈H₈ products observed in *m*-methylbenzyl radical decomposition comprise *p*-xylylene, *o*-xylylene, and 2- and 3-methylfulvenallenes. The *o*- and *p*-xylylenes are formed via the RCMM mechanism depicted in Scheme 2, with the methylfulvenallenes produced via the benzyl decomposition mechanism (Scheme 3). As the most stable xylylene, it is likely that *m*-xylylene rearranges predominantly to *p*-xylylene, while 3-methylfulvenallene is slightly favored energetically over 2-methylfulvenallene. The proposed mechanism for *m*-methylbenzyl radical decomposition to C₈H₈ + H is depicted in Scheme 4.

By analogy to the benzyl isomerization/decomposition mechanism, RCMM isomerization should require a maximum barrier

of 70.3 kcal mol⁻¹. The second isomerization step has the least favorable pre-exponential factor, 3.26 × 10¹³T^{0.128} s⁻¹,⁸ and we have adopted this value for the overall process. This provides the rate expression $k [s^{-1}] = 3.26 \times 10^{13} T^{0.128} \exp(-35400/T)$ for decomposition of *m*-methylbenzyl to *p*-xylylene + H (perhaps with some fraction as *o*-xylylene). Another possible source of C₈H₈ + H in *m*-methylbenzyl radical decomposition is a methylfulvenallene + H (cf. Scheme 3). The overall barrier for decomposition to these products is higher than for *o*/*p*-xylylene + H, but it should be assisted by a relatively large pre-exponential factor for the controlling C–H bond scission reaction, which proceeds without an adiabatic barrier. The barrier for *m*-methylbenzyl decomposition to 3-methylfulvenallene + H is 83.9 kcal mol⁻¹ (formation of the 2-methylfulvenallene isomer is slightly more endothermic, with barrier of 84.1 kcal mol⁻¹). Assuming that the activation energy is equal to the reaction enthalpy, with a pre-exponential factor based upon the work of da Silva et al.,⁸ we estimate that *m*-methylbenzyl decomposes to 3-methylfulvenallene + H according to the rate expression $k [s^{-1}] = 1.26 \times 10^{15} \exp(-42200/T)$. Our estimated rate expressions for the formation of *p*-xylylene + H and 3-methylfulvenallene + H are plotted in Figure 8, where they can be compared to the experimental results. The estimated rate constants for formation of *p*-xylylene + H are in good agreement with the experimental C₈H₈ + H measurements (essentially to

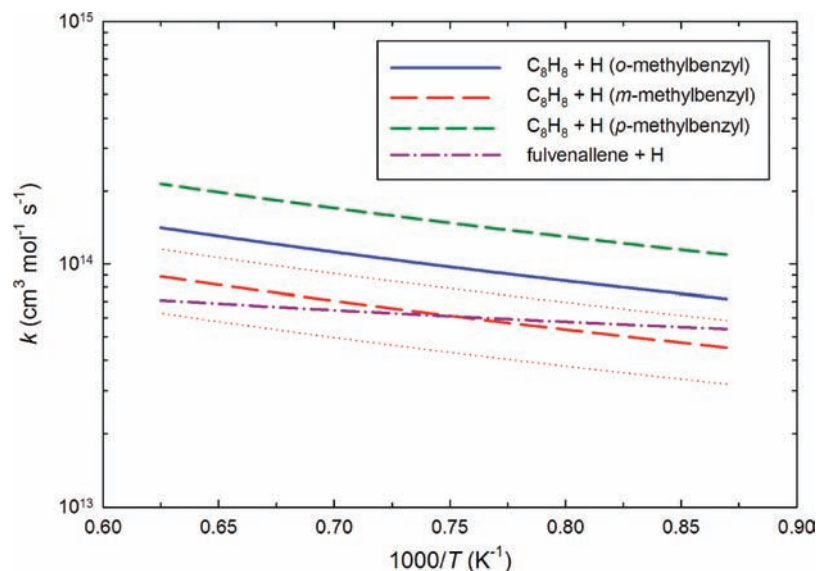


Figure 9. Rate constants for $C_8H_8 + H$ addition, measured in *o*-, *m*-, and *p*-methylbenzyl decomposition experiments,¹¹ compared to variational transition state theory results for the fulvenallene + H reaction.⁸ Experimental uncertainties (dotted lines) included for *m*-methylbenzyl experiments only.

TABLE 4: Estimated Rate Parameters for Reactions in the Methylbenzyl Radical Decomposition Mechanisms^a

	E_a	A
<i>p</i> -methylbenzyl \rightarrow <i>p</i> -xylylene + H	61.5	7.2×10^{14}
<i>p</i> -methylbenzyl \rightarrow fulvenallene + CH_3	76.2	4.0×10^{15}
<i>o</i> -methylbenzyl \rightarrow <i>o</i> -xylylene + H	67.3	1.6×10^{15}
<i>o</i> -methylbenzyl \rightarrow fulvenallene + CH_3	75.5	4.0×10^{15}
<i>m</i> -methylbenzyl \rightarrow <i>m</i> -xylylene + H	88.1	1.1×10^{15}
<i>m</i> -methylbenzyl \rightarrow <i>p</i> -xylylene + H	70.3	$3.26 \times 10^{13} T^{0.128}$
<i>m</i> -methylbenzyl \rightarrow 2-methylfulvenallene + H	83.9	1.26×10^{15}
<i>m</i> -methylbenzyl \rightarrow fulvenallene + CH_3	76.1	4.0×10^{15}

^a E_a in kcal mol⁻¹, A in s⁻¹. High-pressure-limit values.

within experimental error), and we therefore propose that *p*-xylylene + H are actually the major decomposition products of the *m*-methylbenzyl radical. The methylfulvenallene pathway is predicted to play a minor role at low temperatures (2% of the C_8H_8 products at 1000 K), increasing to become a significant product set at higher temperatures (over 30% at 2000 K). While these estimated rate expressions for the formation of *p*-xylylene and 3-methylfulvenallene are in the high-pressure limit, they provide strong evidence that they are the main C_8H_8 products of *m*-methylbenzyl radical decomposition, where it is highly unlikely that *m*-xylylene will form in any meaningful amount.

Again, we include an estimate of the fulvenallene + CH_3 pathway in our consideration of *m*-methylbenzyl radical decomposition. Because this methylbenzyl isomer demonstrates the largest barrier to decomposition, these products are expected to play the greatest role here (although they do not contribute to the experimentally measured decomposition rate). Using our calculated reaction enthalpy of 76.1 kcal mol⁻¹, the rate expression $k [s^{-1}] = 1 \times 10^{15} \exp(-38300/T)$ is estimated, and has been included in Figure 8. We find that decomposition of *m*-methylbenzyl to the C_7H_6 species fulvenallene plus CH_3 is of similar importance to the total decomposition rate to C_8H_8 products + H (the fulvenallene + CH_3 channel comprises 73% of the total reaction flux at 1000 K, and 42% at 2000 K). The different products discerned here for *m*-methylbenzyl radical decomposition versus the ortho isomer, as well as the higher activation energy, may explain the increased ignition delays for *m*- versus *o*-xylene measured by Roubaud et al.³

Some experimental support for fulvenallene and/or methylfulvenallene as significant products in *m*-methylbenzyl pyrolysis

is provided by the results of Fernandez et al.¹² In their pyrolysis studies of the methylbenzyl radicals, rate expressions were fit for the reverse $C_8H_8 + H$ reactions, with significant differences obtained for the three isomers. Rate expressions for the three recombination reactions are plotted in Figure 9, between 1150 and 1600 K, along with high-pressure-limit rate constants for the fulvenallene + H reaction calculated by da Silva et al.⁸ using variational transition state theory (here we are assuming that the methylfulvenallene + H reactions proceed at the same rate, and lump these processes together). The $C_8H_8 + H$ rate constants decrease in the order para > ortho > meta, consistent with increasing formation of fulvenallene/methylfulvenallene. The $C_8H_8 + H$ rate constants obtained in the *m*-methylbenzyl pyrolysis experiments agree with the variational fulvenallene + H values, to within the experimental uncertainty, strengthening our argument that fulvenallene species are important products of *m*-methylbenzyl decomposition. Furthermore, the fitted methylbenzyl + H rate constants follow the same trend as those for $C_8H_8 + H$, perhaps further absorbing some of the fulvenallene + H effect. The *m*-methylbenzyl + H rate constant of $6.3 \times 10^{13} \text{ cm}^3 \text{ mol}^{-1} \text{ s}^{-1}$ is a factor of 5 below that for the well-known benzyl + H reaction ($3.3 \times 10^{14} \text{ cm}^3 \text{ mol}^{-1} \text{ s}^{-1}$),³⁶ whereas the *p*-methylbenzyl + H value is in quite good agreement. The results for $C_8H_8 + H$ and $C_8H_9 + H$ in the *o*-methylbenzyl experiments suggest that fulvenallene and/or methylfulvenallene may also be significant products here. These results may be somewhat coincidental, however, given the relatively narrow range for organic molecule + H and radical + H association rate constants. Further theoretical calculations on the xylylene and methylfulvenallene + H reactions will allow us to better interpret the available experimental data.

The formation of significant quantities of the CH_3 radical in *m*-methylbenzyl decomposition, versus free H atoms for the same reactions in the ortho and para isomers, may also help explain trends in burning velocities. The *o*- and *p*-xylene isomers have peak burning velocities that are essentially the same (ca. 0.61 m s^{-1}), whereas the *m*-xylene peak burning velocity of 0.56 m s^{-1} is significantly slower.¹³ Burning velocities tend to be increased by reactions leading to free H atoms (achieving chain branching via $H + O_2 \rightarrow OH + O$), and decreased by reactions that form the CH_3 radical.¹³ The slower burning

TABLE 5: Recommended Thermochemical Properties^a

	$\Delta_f H^\circ_{298}$	S°_{298}	$C_{P,300}$	$C_{P,400}$	$C_{P,500}$	$C_{P,600}$	$C_{P,800}$	$C_{P,1000}$	$C_{P,1500}$	$C_{P,2000}$
<i>o</i> -xylylene	58.98	79.945	29.275	38.555	46.283	52.510	61.731	68.216	77.962	82.903
<i>m</i> -xylylene (triplet)	79.20	81.744	30.881	40.259	47.902	53.969	62.845	69.052	78.404	83.167
<i>m</i> -xylylene (singlet)	95.89	80.624	31.072	40.255	47.810	53.844	62.712	68.933	78.324	83.113
<i>p</i> -xylylene	52.61	77.706	26.221	38.447	46.155	52.383	61.633	68.148	77.937	82.892
1-methylene-2,4-cyclohexadiene	43.23	78.016	25.845	34.361	41.653	47.614	56.550	62.882	72.408	77.217
1-methylene-2,5-cyclohexadiene	39.86	75.237	25.660	34.180	41.483	47.465	56.449	62.821	72.394	77.217
<i>o</i> -methylbenzyl	43.83	83.924	31.143	40.422	48.327	54.796	64.515	71.432	81.903	87.223
<i>m</i> -methylbenzyl	43.23	85.057	30.295	39.740	47.805	54.395	64.267	71.268	81.831	87.184
<i>p</i> -methylbenzyl	43.17	83.820	30.273	39.707	47.771	54.366	64.253	71.265	81.838	87.192
2-methylfulvenallene	75.23	85.557	30.442	38.930	46.176	52.117	61.075	67.465	77.127	82.022
3-methylfulvenallene	75.02	85.719	30.907	39.304	46.465	52.341	61.216	67.559	77.169	82.045

^a In kcal mol⁻¹ and cal mol⁻¹ K⁻¹.

velocities for *m*-xylene, versus *o*- and *p*-xylenes, have been attributed to lower levels of H atom production,¹³ which is now supported by experiment and theory. However, if this were the only effect, then it would be reasonable to expect *o*-xylene burning velocities that are also slower than those for *p*-xylene, given the significant difference in the activation energies for *o*- and *p*-methylbenzyl decomposition (~6 kcal mol⁻¹). If, however, fulvenallene + CH₃ is a major product set in *m*-methylbenzyl radical decomposition, then the increased production of unreactive CH₃ radicals, at the expense of free H atoms, would significantly reduce *m*-xylene burning velocities. We believe that *m*-xylene burning velocities and ignition behavior will be explained by both the increased stability of the *m*-methylbenzyl radical and the propensity of this species to decompose to CH₃ and H radicals.

3.5.4. Reaction Rate Expressions. Rate parameters for the different reaction processes considered here, estimated using computational chemistry and thermochemical kinetic techniques, are listed in Table 4. Where possible, rate constants have been quoted in the high-pressure limit (in several cases relying on the assignment of the experimental data being 4 times below this limit). The new rate expressions presented here, along with the novel products that have been proposed (with their further oxidation chemistry), should be introduced to kinetic mechanisms in order to improve modeling of xylene oxidation, and other polyalkylated aromatic hydrocarbons.

3.6. Heat Capacity and Entropy Data. In addition to the enthalpies of formation reported here, reliable entropies and heat capacities are also required in kinetic modeling. We have calculated these properties for the target species of this study (fulvenallene is reported elsewhere),⁸ and they are provided in Table 5, along with our best estimates for heats of formation. These results make use of our calculated rotor potentials to account for internal rotational modes.

4. Conclusions

We report thermochemical properties for a variety of hydrocarbons involved in combustion of the xylenes, from the results of high-level theoretical calculations. When we couple our results with thermochemical kinetic approximations, we determine several new, important, product sets in the thermal decomposition of the methylbenzyl radical isomers that form from xylene oxidation and pyrolysis. It is suggested that the *m*-methylbenzyl radical does not decompose to the C₈H₈ product *m*-xylylene (+ H), instead forming *p*-xylylene, with perhaps lesser amounts of methylfulvenallene and *o*-xylylene. It is predicted that fulvenallene + CH₃ are important products of *m*-methylbenzyl decomposition, and that they also play a role in decomposition of the ortho and para isomers.

Acknowledgment. J.W.B. wishes to acknowledge partial support from ExxonMobil funding to education, the U.S. Army Research Office, and a U.S. Air Force STTR contract.

Supporting Information Available: Optimized structures, vibrational frequencies, and G3X and G3SX energies for target molecules; ionization energies for ring compounds; side-on depiction of *o*-xylylene; internal rotor potential for *p*-methylbenzyl. This material is available free of charge via the Internet at <http://pubs.acs.org>.

References and Notes

- (1) (a) Lovell, W. G. *Ind. Eng. Chem.* **1948**, *40*, 2388. (b) American Petroleum Institute Research Project 45. *Knocking Characteristics of Pure Hydrocarbons*; American Society for Testing Materials, 1958.
- (2) Shen, H.-P. S.; Oehlschlaeger, M. A. *Combust. Flame* **2009**, *156*, 1053.
- (3) Roubaud, A.; Minetti, R.; Sochet, L. R. *Combust. Flame* **2000**, *121*, 535.
- (4) da Silva, G.; Chen, C.-C.; Bozzelli, J. W. *J. Phys. Chem. A* **2007**, *111*, 8663.
- (5) da Silva, G.; Bozzelli, J. W. *J. Phys. Chem. A* **2007**, *111*, 7987.
- (6) da Silva, G.; Bozzelli, J. W. *J. Phys. Chem. A* **2008**, *112*, 3566.
- (7) da Silva, G.; Bozzelli, J. W. *Proc. Combust. Inst.* **2009**, *32*, 287.
- (8) da Silva, G.; Cole, J. A.; Bozzelli, J. W. *J. Phys. Chem. A* **2009**, *113*, 6111.
- (9) da Silva, G.; Bozzelli, J. W. *J. Phys. Chem. A* **2009**, *113*, 6979.
- (10) da Silva, G.; Bozzelli, J. W. *J. Phys. Chem. A* **2009**, *113*, 8971.
- (11) DaCosta, I.; Eng, R. A.; Gilbert, A.; Hippler, H. *Proc. Combust. Inst.* **2000**, *28*, 1537.
- (12) Fernandes, R. X.; Gebert, A.; Hippler, H. *Proc. Combust. Inst.* **2002**, *29*, 1337.
- (13) (a) Johnston, R. J.; Farrell, J. T. *Proc. Combust. Inst.* **2005**, *30*, 217. (b) Farrell, J. T.; Johnston, R. J.; Androulakis, I. P. *SAE Pap.* **2004**, *2004-01-2936*.
- (14) (a) Jones, J.; Bacskay, G. B.; Mackie, J. C. *J. Phys. Chem. A* **1997**, *101*, 7105. (b) Oehlschlaeger, M. A.; Davidson, D. F.; Hanson, R. K. *J. Phys. Chem. A* **2006**, *110*, 6649.
- (15) Cavallotti, C.; Derudi, M.; Rota, R. *Proc. Combust. Inst.* **2009**, *32*, 115.
- (16) Frisch, M. J.; Trucks, G. W.; Schlegel, H. B.; Scuseria, G. E.; Robb, M. A.; Cheeseman, J. R.; Montgomery, J. A., Jr.; Vreven, T.; Kudin, K. N.; Burant, J. C.; Millam, J. M.; Iyengar, S. S.; Tomasi, J.; Barone, V.; Mennucci, B.; Cossi, M.; Scalmani, G.; Rega, N.; Petersson, G. A.; Nakatsuji, H.; Hada, M.; Ehara, M.; Toyota, K.; Fukuda, R.; Hasegawa, J.; Ishida, M.; Nakajima, T.; Honda, Y.; Kitao, O.; Nakai, H.; Klene, M.; Li, X.; Knox, J. E.; Hratchian, H. P.; Cross, J. B.; Adamo, C.; Jaramillo, J.; Gomperts, R.; Stratmann, R. E.; Yazyev, O.; Austin, A. J.; Cammi, R.; Pomelli, C.; Ochterski, J. W.; Ayala, P. Y.; Morokuma, K.; Voth, G. A.; Salvador, P.; Dannenberg, J. J.; Zakrzewski, V. G.; Dapprich, S.; Daniels, A. D.; Strain, M. C.; Farkas, O.; Malick, D. K.; Rabuck, A. D.; Raghavachari, K.; Foresman, J. B.; Ortiz, J. V.; Cui, Q.; Baboul, A. G.; Clifford, S.; Cioslowski, J.; Stefanov, B. B.; Liu, G.; Liashenko, A.; Piskorz, P.; Komaromi, I.; Martin, R. L.; Fox, D. J.; Keith, T.; Al-Laham, M. A.; Peng, C. Y.; Nanayakkara, A.; Challacombe, M.; Gill, P. M. W.; Johnson, B.; Chen, W.; Wong, M. W.; Gonzalez, C.; Pople, J. A. *Gaussian 03*, Revision D.01; Gaussian, Inc.: Wallingford, CT, 2004.
- (17) Curtiss, L. A.; Redfern, P. C.; Raghavachari, K.; Pople, J. A. *J. Chem. Phys.* **2001**, *114*, 108.

- (18) Chase, M. W., Jr. *J. Phys. Chem. Ref. Data, Monogr.* **1998**, 9, 1.
- (19) (a) Raghavachari, K.; Stefanov, B. B.; Curtiss, L. A. *J. Chem. Phys.* **1997**, 106, 6764. (b) da Silva, G.; Bozzelli, J. W. *J. Chem. Phys. A* **2006**, 110, 12977. (c) da Silva, G.; Sebbar, N.; Bozzelli, J. W.; Bockhorn, H. *ChemPhysChem* **2006**, 7, 1119.
- (20) (a) Ruscic, B.; Pinzon, R. E.; Morton, M. L.; von Laszewski, G.; Bittner, S. J.; Nijssure, S. G.; Amin, K. A.; Minkoff, M.; Wagner, A. F. *J. Phys. Chem. A* **2004**, 108, 9979. (b) Ruscic, B. *Unpublished results from Active Thermochemical Tables v.1.25 using the Core (Argonne) Thermochemical Network*, 2005, v. 1.049.
- (21) Prosen, E. J.; Johnson, W. H.; Rossini, F. D. *J. Res. Natl. Bur. Stand. (U.S.)* **1946**, 36, 455.
- (22) Bartmess, J. E. *J. Am. Chem. Soc.* **1982**, 104, 335.
- (23) Bally, T.; Hasselmann, D.; Loosen, K. *Helv. Chim. Acta* **1985**, 68, 345.
- (24) Lories, X.; Vandooren, J.; Peeters, D. *Chem. Phys. Lett.* **2008**, 452, 29.
- (25) Pollack, S. K.; Raine, B. C.; Hehre, W. J. *J. Am. Chem. Soc.* **1981**, 103, 6308.
- (26) Roth, W. R.; Scholz, B. P. *Chem. Ber.* **1981**, 114, 3741.
- (27) Hammad, L. A.; Wenthold, P. G. *J. Am. Chem. Soc.* **2000**, 122, 11203.
- (28) Hayashibara, K.; Kruppa, G. H.; Beauchamp, J. L. *J. Am. Chem. Soc.* **1986**, 108, 5441.
- (29) Ruscic, B.; Pinzon, R. E.; Morton, M. L.; von Laszewski, G.; Bittner, S. J.; Nijssure, S. G.; Amin, K. A.; Minkoff, M.; Wagner, A. F. *J. Phys. Chem. A* **2004**, 108, 9979.
- (30) Karton, A.; Kaminker, I.; Martin, J. M. L. *J. Phys. Chem. A* **2009**, 113, 7610.
- (31) (a) Davico, G. E.; Bierbaum, V. M.; DePuy, C. H.; Ellison, G. B.; Squires, R. R. *J. Am. Chem. Soc.* **1995**, 117, 2590. (b) Alecu, I. M.; Gao, Y.; Hsieh, P.-C.; Sand, J. P.; Ors, A.; McLeod, A.; Marshall, P. J. *J. Phys. Chem. A* **2007**, 111, 3970.
- (32) Poutsma, J. C.; Nash, J. J.; Paulino, J. A.; Squires, R. R. *J. Am. Chem. Soc.* **1997**, 119, 4686.
- (33) (a) Braun-Unkhoff, M.; Frank, P.; Just, T. *Ber. Bunsen-Ges. Phys. Chem.* **1990**, 94, 1417. (b) Sivaramakrishnan, R.; Tranter, R. S.; Brezinsky, K. *J. Phys. Chem. A* **2006**, 110, 9400.
- (34) Ruscic, B.; Litorja, M.; Asher, R. L. *J. Phys. Chem. A* **1999**, 103, 8625.
- (35) Oehlschlaeger, M. A.; Davidson, D. F.; Hanson, R. K. *Proc. Combust. Inst.* **2007**, 31, 211.
- (36) Baulch, D. L.; Cobos, C. J.; Cox, R. A.; Esser, C.; Frank, P.; Just, T.; Kerr, J. A.; Pilling, M. J.; Troe, J.; Walker, R. W.; Warnatz, J. *J. Phys. Chem. Ref. Data* **1992**, 21, 411.

JP905722T